Inter-Period Correlation of Acceleration Response Spectra in Observed and Simulated Ground Motions

T. Itoi
Department of Nuclear Engineering and Management, Graduate School of Engineering, The University of Tokyo, Japan

T. Takada
Department of Architecture, Graduate School of Engineering, The University of Tokyo, Japan

SUMMARY:
A methodology is proposed to model an empirical correlation model between acceleration response spectra of ground motions at different periods for a ground motion prediction equation. The proposed method distinguishes inter-event and intra-event residuals. Difference between inter-event correlation structure, which is due to uncertainty in seismic source characteristics, and intra-event correlation characteristics, which is from propagation path and site characteristics, is discussed. The factor affecting correlation of intra-event residual is investigated by ground motion simulation considering deep subsurface structure.

Keywords: Ground motion prediction equation, acceleration response spectrum, correlation

1. INTRODUCTION

Empirical correlation models between acceleration response spectra of ground motions at different periods were proposed for ground motion prediction equations (Inoue, 1990; Baker & Cornell, 2006; Wang, 2007; Tanaka *et al*., 2008; Baker & Jayaram, 2008; Jayaram *et al*., 2011). These models are widely used for probabilistic assessment of simultaneous collapse of multiple structures (e.g. Wang *et al*., 2009), as well as for seismic response analyses of multi-degree-of-freedom structure (e.g. Inoue, 1990).

The correlation models in preceding studies were proposed based on ground motions recorded at stations with different site conditions from various types of earthquakes. These correlation models were constructed for total residual of ground motions. In this study, correlation structures for inter-event and intra-event residuals are investigated separately. Then, physical property for the correlation structure is briefly discussed.

2. GROUND MOTION PREDICTION EQUATION AND CORRELATION STRUCTURE

Acceleration response spectrum of ground motion is predicted using a ground motion prediction equation as follows:

$$\log S_A(T) = \log\overline{S_A}(T) + \varepsilon_{total}(T) = \log\overline{S_A}(T) + \varepsilon_{Intra}(T) + \varepsilon_{Inter}(T) \quad (1)$$

Where, $S_A(T)$ is geometric mean acceleration response spectrum of two orthogonal horizontal components. $\overline{S_A}(T)$ is median response spectrum predicted by a ground motion prediction equation; median response spectrum at engineering bedrock sites calculated by Uchiyama & Midorikawa (2006) is used in this study. $\varepsilon_{total}(T)$, $\varepsilon_{Intra}(T)$ and $\varepsilon_{Inter}(T)$ are zero-mean random variables, which are total residual, intra-event residual and inter-event residual respectively with zero mean. $\varepsilon_{Intra}(T)$ and $\varepsilon_{Inter}(T)$ are mutually independent.

Variance of response spectrum is composed of variance of inter- and intra-event residuals as follows:

$$\mathrm{Var}[S_A(T)] = {\sigma_{total}}^2(T) = \mathrm{Var}[\varepsilon_{Inter}(T) + \varepsilon_{Intra}(T)]$$
$$= \mathrm{Var}[\varepsilon_{Inter}(T)] + \mathrm{Var}[\varepsilon_{Intra}(T)] = {\sigma_{Inter}}^2(T) + {\sigma_{Intra}}^2(T) \quad (2)$$

Similarly, covariance of response spectra between different periods is calculated as follows:

$$\mathrm{Cov}[S_A(T_1), S_A(T_2)] = \rho_{total}(T_1,T_2)\sigma_{total}(T_1)\sigma_{total}(T_2)$$
$$= \mathrm{Cov}[\varepsilon_{Inter}(T_1) + \varepsilon_{Intra}(T_1), \varepsilon_{Inter}(T_2) + \varepsilon_{Intra}(T_2)]$$
$$= \mathrm{Cov}[\varepsilon_{Inter}(T_1), \varepsilon_{Inter}(T_2)] + \mathrm{Cov}[\varepsilon_{Intra}(T_1), \varepsilon_{Intra}(T_2)] \quad (3)$$
$$= \rho_{inter}(T_1,T_2)\sigma_{inter}(T_1)\sigma_{inter}(T_2) + \rho_{intra}(T_1,T_2)\sigma_{intra}(T_1)\sigma_{intra}(T_2)$$

Where, $\rho_{inter}(T_1,T_2)$ is the correlation coefficient between $\varepsilon_{Inter}(T_1)$ and $\varepsilon_{Inter}(T_2)$, while $\rho_{intra}(T_1,T_2)$ is the correlation coefficient between $\varepsilon_{Intra}(T_1)$ and $\varepsilon_{Intra}(T_2)$.

Inter-event residual $\varepsilon_{Inter}(T)$ is considered to stem from uncertainty in source parameters, while intra-event residual $\varepsilon_{Intra}(T)$ depends mainly on uncertainty in site amplification, propagation path characteristics (Midorikawa & Ohtake, 2003; Strasser & Bommer, 2005). Therefore, by dividing total residual into inter- and intra-event residuals as in Equations (2) and (3), factors affecting variability and correlation can be briefly identifiable. According to Anderson & Uchiyama (2011), uncertainty in site amplification and path characteristics can be eliminated from $\varepsilon_{Intra}(T)$ by utilizing a site- and path-specific prediction equation.

3. CORRELATION IN OBSERVED GROUND MOTION ACCERELATION RESPONSE SPECTRA

3.1. Selected Earthquakes and Observation Stations

Ground motions observed during 19 ($= m_T$) aftershocks (M_J > 5.0) are used in this study, which occurred after 2004 Niigata-ken Chuetsu Earthquake (M_J= 6.8). Ground motions recorded at K-NET and KiK-net stations are selected based on the following two criteria; i) peak horizontal acceleration is less than 200 cm/s^2 to exclude the nonlinear site amplification effects, ii) hypocenter distance is less than 100 km, since ground motions exhibit different characteristics from around this distance range. Epicenters of these aftershocks are shown in **Figure 1** and **Table 1** shows the list of earthquakes. Since epicenters of the aftershocks are close to each other, event-to-event difference in source-to-site azimuth, which affects the magnitude of intra-event residual (Strasser & Bommer, 2005; Itoi *et al*., 2009), is considered small.

3.2. Residual in Ground Motion Prediction Equation

3.2.1. Residual Variance

Residual of response spectrum for the *i*-th earthquake at the *j*-th station $\delta_{ij}(T)$ is calculated as follows:

$$\delta_{ij}(T) = \log S^{ij}_{\mathrm{Aobs}}(T) - \log\overline{S^{ij}_A}(T) \quad (4)$$

Where, $S^{ij}_{\mathrm{Aobs}}(T)$ is an observed acceleration spectrum for the *i*-th earthquake at the *j*-th station and $\overline{S^{ij}_A}(T)$ is the predicted acceleration spectrum. $\log X$ is the natural logarithm of X.

Root mean square of the residuals for all records is shown in **Figure 4** (a), which is calculated as follows:

$$\sigma_{total}(T) = \sqrt{\frac{1}{N}\sum_{i,j}{\delta_{ij}}^2(T)} \quad (5)$$

Where, $N\ (= 71)$ is a total number of data as follows:

$$N = \sum_j m_j = \sum_i n_i \quad (6)$$

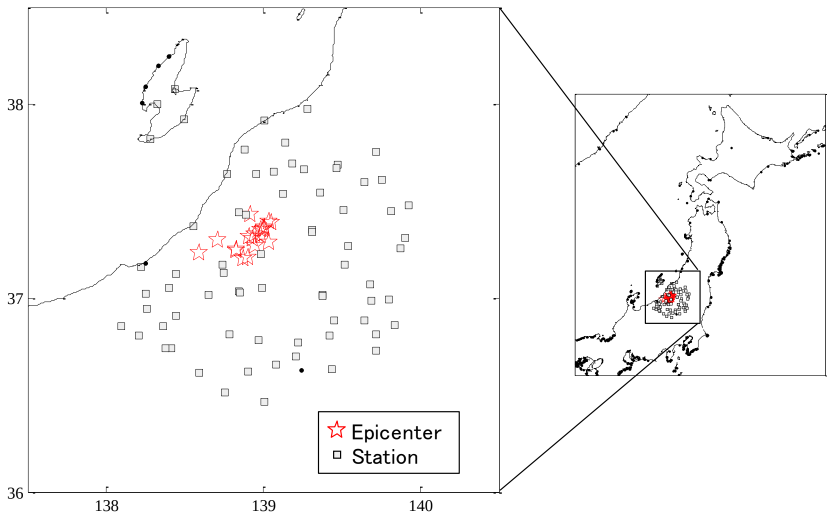

Figure 1. Location of epicenters and K-NET and KiK-net stations

Table 1. List of aftershocks used in this study

EQ No.	yyyy/mm/dd	hh:mm:ss	latitude	longitude	depth (km)	M_J	M_W (F-NET)	M_W (USGS)	M_W (mean)
1	2004/10/23	18:03:13	37.3510	138.9865	9.38	6.3	5.9	6.1	6.00
2	2004/10/23	18:11:57	37.2500	138.8327	11.52	6.0	5.7	5.8	5.75
3	2004/10/23	18:34:06	37.3033	138.9332	14.17	6.5	6.3	6.3	6.30
4	2004/10/23	21:44:28	37.2698	138.9462	14.64	5.0	4.9	5.2	5.05
5	2004/10/23	23:34:46	37.3140	138.9090	19.88	5.3	5.0	5.2	5.10
6	2004/10/24	14:21:35	37.2420	138.8293	11.49	5.0	4.7	4.8	4.75
7	2004/10/25	00:28:09	37.1995	138.8738	10.08	5.3	5.1	5.2	5.15
8	2004/10/25	06:04:58	37.3270	138.9500	15.20	5.8	5.6	5.7	5.65
9	2004/10/27	10:40:50	37.2888	139.0365	11.60	6.1	5.8	6.0	5.90
10	2004/11/1	04:35:49	37.2088	138.9040	8.49	5.0	4.8	4.8	4.80
11	2004/11/4	08:57:30	37.4273	138.9188	18.02	5.2	5.1	5.3	5.20
12	2004/11/6	02:53:21	37.3593	139.0048	0.22	5.1	4.9	5.1	5.00
13	2004/11/8	11:15:59	37.3930	139.0352	0.00	5.9	5.5	5.5	5.50
14	2004/11/8	11:32:17	37.3883	139.0500	5.85	5.1	4.8	4.9	4.85
15	2004/11/9	04:16:00	37.3510	139.0025	0.00	5.0	4.6	4.9	4.75
16	2004/11/10	03:43:08	37.3667	139.0038	4.55	5.3	5.1	5.1	5.10
17	2004/12/28	18:30:37	37.3193	138.9858	8.11	5.0	4.7	4.8	4.75
18	2005/6/20	13:03:13	37.2293	138.5907	14.51	5.0	4.9	4.9	4.90
19	2005/8/21	11:29:30	37.2983	138.7118	16.73	5.0	4.6	4.8	4.70

Where, m_j is a number of earthquakes which triggered the seismometer at the *j*-th station, and n_i is a number of records observed during the *i*-th earthquake, respectively.

Mean residual of the *i*-th earthquake for all stations $\bar{\delta}_i(T)$ is calculated as follows:

$$\bar{\delta}_i(T) = \frac{1}{n_i}\sum_j \delta_{ij}(T) \tag{7}$$

Where, $n_i(\leq n_T)$ is a number of records observed at the station during the *i*-th earthquake. Residuals $\delta_{ij}(T)$ and mean residual $\bar{\delta}_i(T)$ for earthquakes (No. 1 and 3 in **Table 1**) are shown in **Figure 2**, which are different from each other. Mean residual for all records $\bar{\delta}(T)$ is calculated as follows:

$$\bar{\delta}(T) = \frac{1}{N}\sum_{i,j} \delta_{ij}(T) \tag{8}$$

Inter-event residual of the *i*-th earthquake $\overline{\delta^i_{inter}}(T)$ is assumed to be calculated as follows:

$$\overline{\delta^i_{inter}}(T) = \bar{\delta}_i(T) - \bar{\delta}(T) \tag{9}$$

Standard deviation of inter-event residual for all earthquakes is shown later in **Figure 4** (a), which is calculated as follows:

$$\sigma_{inter}(T) = \sqrt{\frac{1}{m_T}\sum_i \left(\overline{\delta^i_{inter}}(T) - \overline{\delta_{inter}}(T)\right)^2} \tag{10}$$

Intra-event residual is calculated. Stations are selected where more than ten records were observed out of 19 earthquakes. First, intra-event residual from the source-specific prediction equation for the *i*-th earthquake at the *j*-th station $\delta_{ij\mathrm{I}}(T)$ is shown in **Figure 3**, which is calculated as follows:

$$\delta_{ij\mathrm{I}}(T) = \log S^{ij}_{A\mathrm{obs}}(T) - \log \overline{S^{ij}_A}(T) - \overline{\delta^i_{inter}}(T) \tag{11}$$

Root mean square of intra-event residual at the *j*-th station is calculated as follows:

$$\sigma^j_{intra\mathrm{I}}(T) = \sqrt{\frac{1}{m_j}\sum_i {\delta_{ij\mathrm{I}}}^2(T)} \tag{12}$$

Root mean square of intra-event residual for all records is shown in **Figure 4** (a), which is calculated as follows:

$$\sigma_{intra\mathrm{I}}(T) = \sqrt{\frac{1}{N}\sum_{i,j} {\delta_{ij\mathrm{I}}}^2(T)} \tag{13}$$

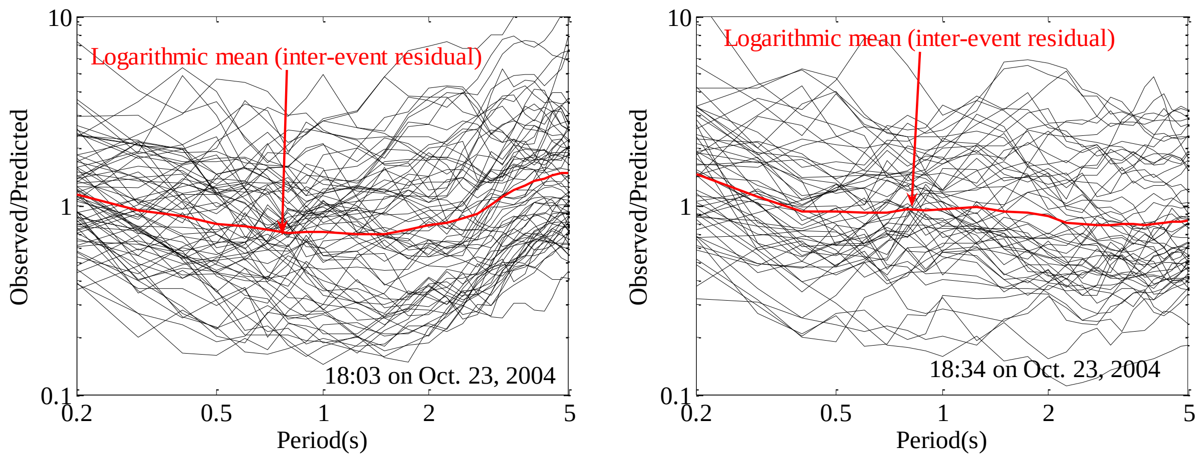

(a) EQ No. 1 (b) EQ No. 3

Figure 2. Examples of inter-event residual

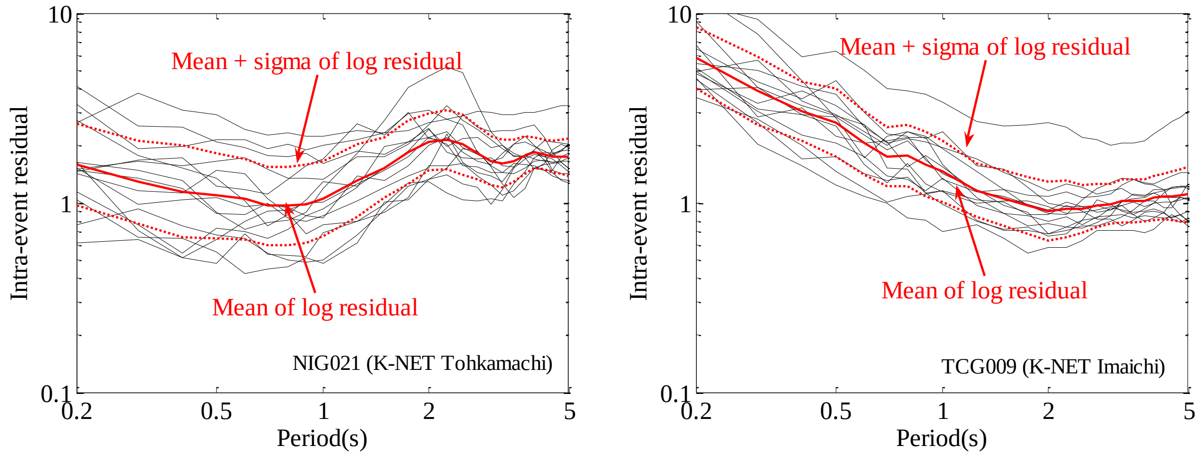

(a) NIG021 (K-NET Tohkamachi) (b) TCG009 (K-NET Imaichi)

Figure 3. Examples of intra-event residual

Mean residual at the *j*-th station for all earthquakes is used as correction term for site amplification at the *j*-th station, which is calculated as follows:

$$\overline{\delta_{intra\mathrm{I}}^{j}}(T) = \frac{1}{m_j}\sum_{i}\delta_{ij\mathrm{I}}(T) \tag{14}$$

For site- and source-specific ground motion prediction, intra-event residual is calculated similar to Eq (11) as follows:

$$\delta_{ij\mathrm{II}}(T) = \log S_{A\mathrm{obs}}^{ij}(T) - \log\overline{S_{A}^{ij}}(T) - \overline{\delta_{inter}^{i}}(T) - \overline{\delta_{intra\mathrm{I}}^{j}}(T) \tag{15}$$

Then, root mean square of updated intra-event residual for earthquakes at the *j*-th station is as follows:

$$\sigma_{intra\mathrm{II}}^{j}(T) = \sqrt{\frac{1}{m_j}\sum_{i}{\delta_{ij\mathrm{II}}}^{2}(T)} \; \left(\le \sigma_{intra\mathrm{I}}^{j}(T)\right) \tag{16}$$

Root mean square of updated intra-event residual for all records as follows:

$$\sigma_{intra\mathrm{II}}(T) = \sqrt{\frac{1}{N}\sum_{i,j}{\delta_{ij\mathrm{II}}}^{2}(T)} \; \left(\le \sigma_{intra\mathrm{I}}(T)\right) \tag{17}$$

Figure 4 (a) compares σ_{total}, σ_{inter}, $\sigma_{intra\mathrm{I}}$ and $\sigma_{intra\mathrm{II}}$. Intra-event residual $\sigma_{intra\mathrm{I}}$ is dominant in total residual σ_{total} before correcting site amplification. Introducing correction term for site amplification decreases intra-event residual (from $\sigma_{intra\mathrm{I}}$ to $\sigma_{intra\mathrm{II}}$) by approximately half. Revised intra-event residual $\sigma_{intra\mathrm{II}}$ is comparable to and slightly larger than inter-event residual σ_{inter}. Increase in intra-event residual $\Delta\sigma_{intra}$ due to difference in site amplification is shown in **Figure 4** (b), which is calculated as follows:

$$\Delta\sigma_{intra} = \sqrt{{\sigma_{intra\mathrm{I}}}^{2}(T) - {\sigma_{intra\mathrm{II}}}^{2}(T)} \tag{18}$$

3.2.2. Correlation between Response Spectra of Different Periods

Correlation coefficient of inter-event residuals at different periods is shown in **Figure 5**, which is calculated as follows:

$$\rho_{inter}(T_1, T_2) = \frac{\sum_i\left(\overline{\delta_{inter}^{i}}(T_1)\cdot\overline{\delta_{inter}^{i}}(T_2)\right)}{\sqrt{\sum_i\left(\overline{\delta_{inter}^{i}}^{2}(T_1)\right)\cdot\sum_i\left(\overline{\delta_{inter}^{i}}^{2}(T_2)\right)}} \tag{19}$$

Correlation at shorter period (T<1s) decays slower compared with that at longer period (T>1s), which suggests that some source parameters, such as stress drop, control the amplitude of acceleration response spectra at shorter period.

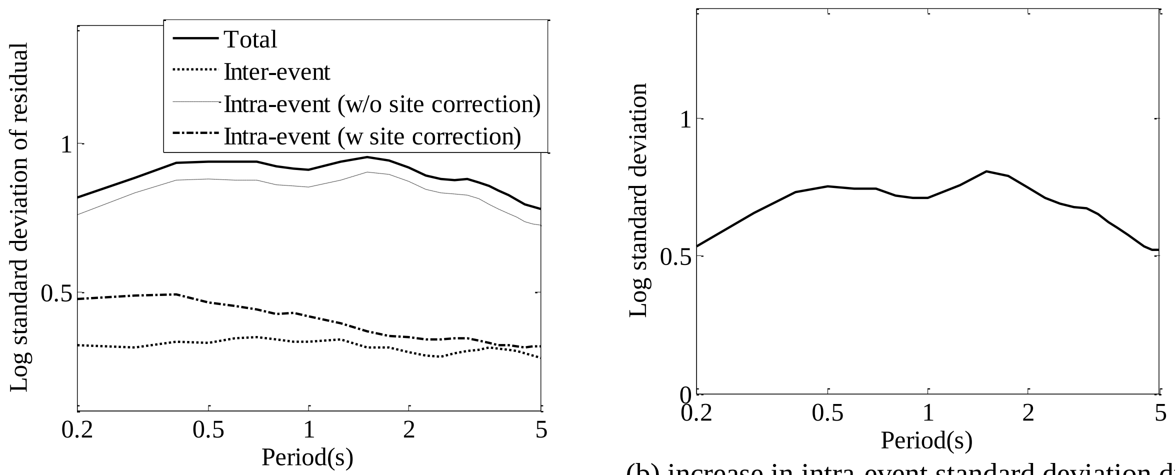

(a)

(b) increase in intra-event standard deviation due to site effects

Figure 4. Standard deviation of logarithmic residual

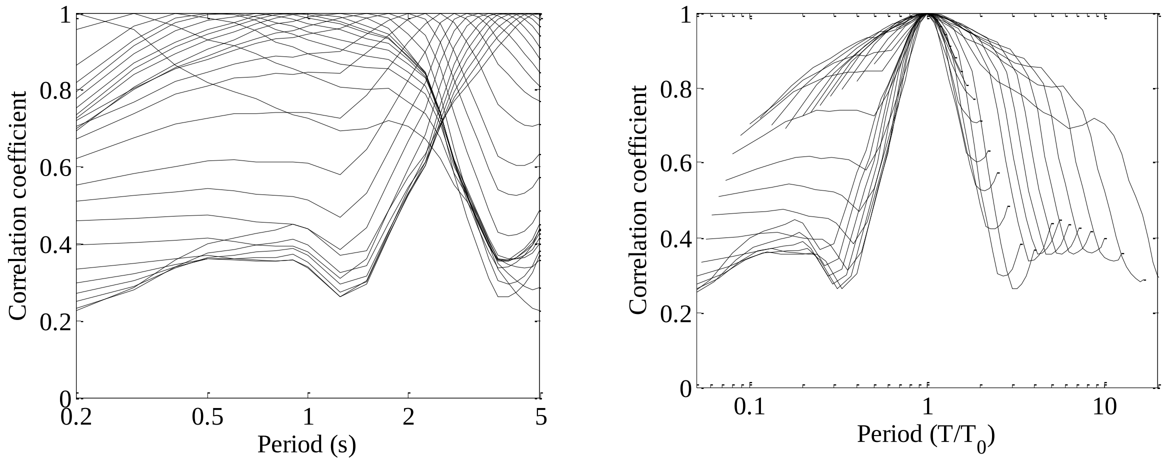

(a) (b)

Figure 5. Correlation coefficient between inter-event residuals

Correlation coefficient of intra-event residuals before site correction is shown in **Figure 6**, which is calculated as follows:

$$\rho_{intra\mathrm{I}}(T_1, T_2) = \frac{\sum_{i,j}\left(\delta_{ij\mathrm{I}}(T_1)\cdot\delta_{ij\mathrm{I}}(T_2)\right)}{\sqrt{\sum_{i,j}\left({\delta_{ij\mathrm{I}}}^2(T_1)\right)\cdot\sum_{i,j}\left({\delta_{ij\mathrm{I}}}^2(T_2)\right)}} \qquad (20)$$

Correlation for shorter period ($T<T_0$) exhibit convex upward curve, while that for longer period ($T>T_0$) shows convex downward characteristics as shown in **Figure 6** (b).

Correlation coefficient of intra-event residuals at different period after site correction is shown in **Figure 7**, which is calculated similarly to Eq. (20) as follows:

$$\rho_{intra\mathrm{II}}(T_1, T_2) = \frac{\sum_{i,j}\left(\delta_{ij\mathrm{II}}(T_1)\cdot\delta_{ij\mathrm{II}}(T_2)\right)}{\sqrt{\sum_{i,j}\left({\delta_{ij\mathrm{II}}}^2(T_1)\right)\cdot\sum_{i,j}\left({\delta_{ij\mathrm{II}}}^2(T_2)\right)}} \qquad (21)$$

Correlation structure of intra-event residual after site correction exhibits almost identical with different periods.

3.2.3. Pseudo-Correlation Caused by Station-to-Station Difference in Site Amplification

As shown in **Figure 4** (b), intra-event residual decreases if site-specific correction term for ground motion prediction equation is introduced. Correlation characteristics of this difference in residuals are evaluated and shown in **Figure 8**, which is calculated as follows:

$$\rho_{\Delta intra}(T_1, T_2) = \frac{\rho_{intra\mathrm{I}}(T_1, T_2)\sigma_{intra\mathrm{I}}(T_1)\sigma_{intra\mathrm{I}}(T_2) - \rho_{intra\mathrm{II}}(T_1, T_2)\sigma_{intra\mathrm{II}}(T_1)\sigma_{intra\mathrm{II}}(T_2)}{\Delta\sigma_{intra}(T_1)\Delta\sigma_{intra}(T_2)} \qquad (22)$$

The correlation characteristics of $\rho_{\Delta intra}$ is similar to that of $\rho_{intra\mathrm{I}}$. This correlation is considered due to station-to-station variation in site amplification, which is not included in a ground motion prediction equation. Site amplification is decomposed into amplification due to shallow and deep subsurface structure. In the following study, the effect of deep subsurface structure on inter-period correlation is evaluated using ground motion simulation.

Figure 9 shows a cross-section of the deep subsurface structure all over Japan, which is based on the model proposed by Fujiwara *et al.* (2009). Site amplification of ground motion is evaluated all over Japan using multiple layer reflection theory (Itoi & Takada, 2012) to evaluate inter-period correlation. **Figure 10** shows the amplification of response spectrum at T = 3s, where similar spatial variation is obtained for different periods. The effect of deep subsurface structure on ground motion shown in **Figure 10** is not considered explicitly in the conventional prediction models. **Figure 11** shows

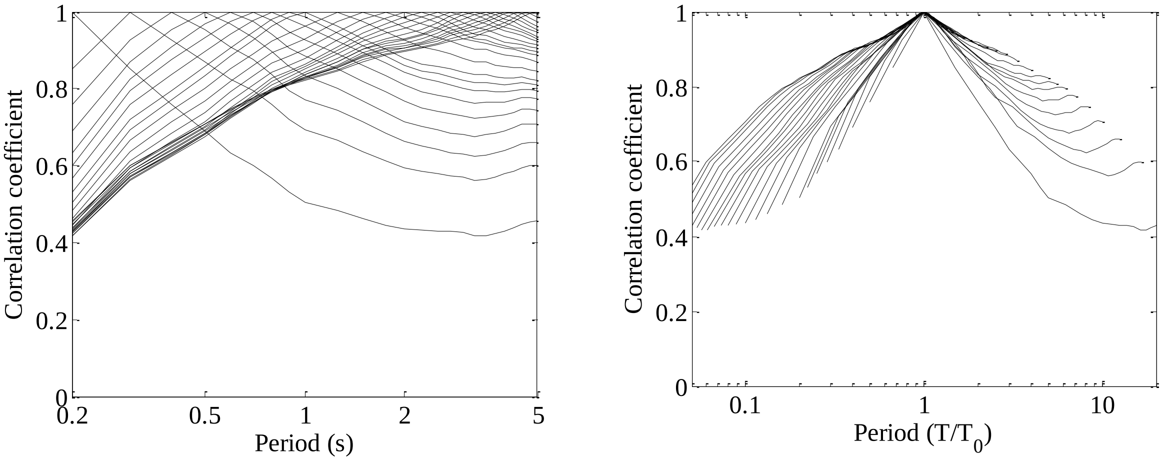

(a) (b)

Figure 6. Correlation coefficient between intra-event residuals (before site correction)

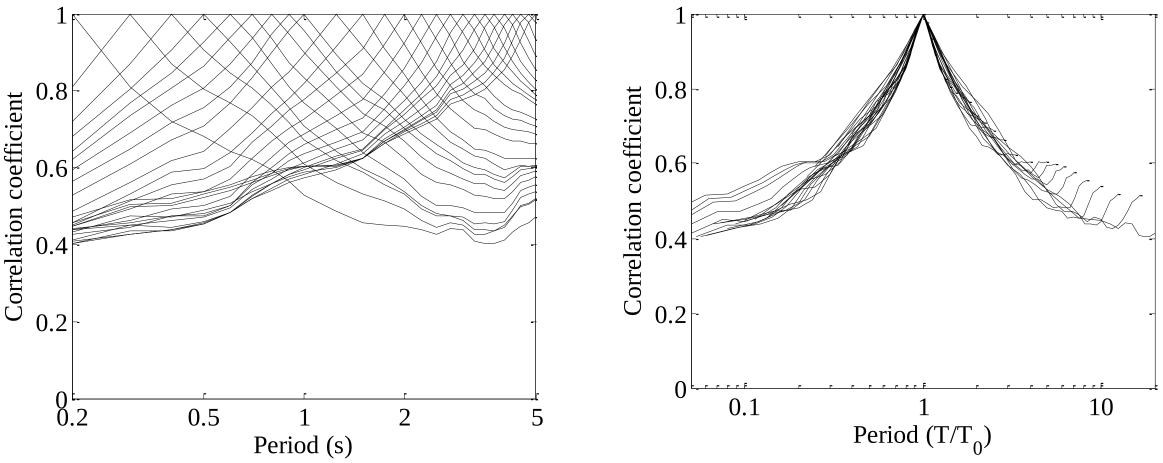

(a) (b)

Figure 7. Correlation coefficient between intra-event residuals (after site correction)

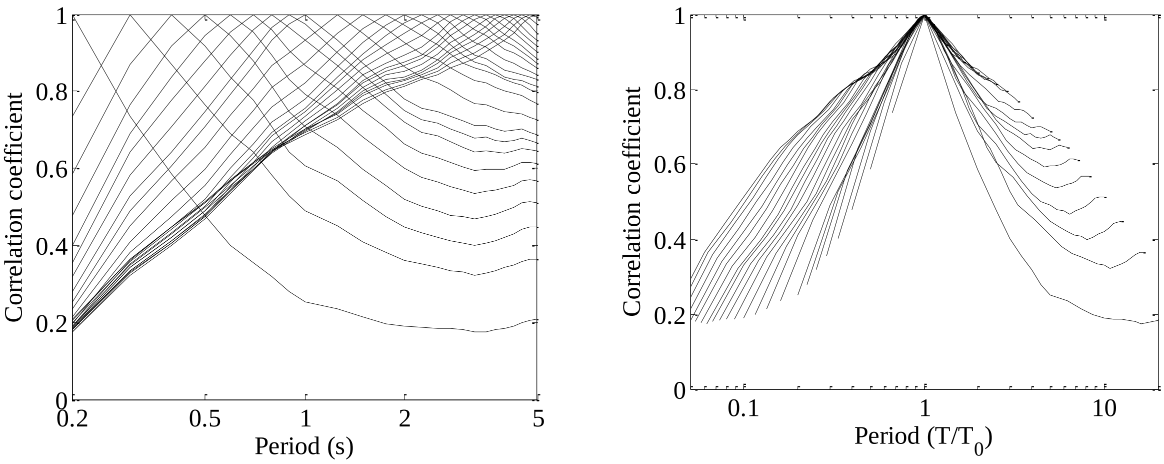

(a) (b)

Figure 8. Pseudo-correlation due to spatial difference in subsurface amplification

the standard deviation, which is about as half as $\Delta\sigma_{intra}$ shown in **Figure 4** (b). The effect of shallow subsurface structure should be included for better correspondence. **Figure 12** shows the correlation coefficient. Though the correlation coefficient is slightly larger than $\rho_{\Delta intra}$ shown in **Figure 8**, they are similar to each other.

4. CONCLUDING REMARKS

An empirical correlation model between acceleration response spectra of ground motions at different periods was proposed for a ground motion prediction equation by analysing aftershock records of 2004 Niigata-Ken Chuetsu Earthquake. The method proposed in this study evaluates the correlation characteristics for inter-event and intra-event residuals separately. Inter-event correlation structure, which is due to uncertainty in seismic source characteristics, is different from intra-event correlation characteristics, which is from propagation path and site characteristics. By introducing correction term for site amplification, the variability of intra-event residual decreased and the correlation characteristics of response spectra changed, which should be introduced in modelling the correlation structure.

AKCNOWLEDGEMENT

Strong ground motion records of K-NET and KiK-net, and moment tensor catalogue of F-net provided by National Research Institute for Earth Science and Disaster Prevention (NIED) of Japan were used in the study.

REFERENCES

Anderson, J. and Uchiyama, Y. (2011). A methodology to Improve Ground-Motion Prediction Equations by Including Path Collections, *Bulletin of the Seismological Society of America*, **101: 4**, 1822-1846.

Baker, J. W. and Cornell, C.A. (2006). Correlation of Response Spectral Values for Multicomponent Ground Motions, *Bulletin of the Seismological Society of America*, **96: 1**, 245-227.

Baker, J. W. and Jayaram, N. (2008). Correlation of Spectral Acceleration Values from NGA Ground Motion Models, *Earthquake Spectra*, **24: 1**, 299-317.

Fujiwara, H., Kawai, S., Aoi, S., Morikawa, N., Senna S., Kudo, N., Ooi, M., Hao, K. H-S., Hayakawa, Y., Toyama, N., Matsuyama, H., Iwamoto, K., Suzuki, H., Liu, Y. (2009). A Study on Subsurface Structure Model for Deep Sedimentary Layers of Japan for Strong-motion Evaluation, *Technical Note of the National Research Institute for Earth Science and Disaster Prevention*, **337**. (in Japanese)

Inoue, T.. (1990). Seismic Hazard Analysis of Multi-Degree-of-Freedom Structures, RMS-8, Stanford, CA.

Itoi, T. Midorikawa, S., Kito, J., Miura, H., Uchiyama, Y., Sakamoto, S. (2009). Variability in Response Spectra for Crustal Earthquake using Stochastic Green's Function Approach, *Journal of Japan Association for Earthquake Engineering*, **9: 1**, 1_128-1_142. (in Japanese with English abstract)

Itoi, T. and Takada, T. (2011). Empirical Correction of Ground Motion Prediction Equations of Response Spectra at Rock Sites for Near-Field Earthquakes Considering Amplification Effect within Deep Subsurface Structure, *Journal of Japan Association for Earthquake Engineering*, **12: 1**, 1_43-1_61. (in Japanese with English abstract)

Itoi, T. and Takada, T. (2012). Macro-Spatial and Inter-Period Correlation of Spectral Acceleration found in Simulated Ground Motion, *Proceedings of the 5th Asian-Pacific Symposium on Structural Reliability and its Applications Sustainable Civil Infrastructures*, May 23 - 35 , 2012, Singapore. (in press)

Jayaram, N., Baker, J. W., Okano, H., Ishida, H., McCann, Jr., M. W. and Mihara, Y. (2011). Correlation of Response Spectral Values in Japanese Ground Motions, *Earthquakes and Structures*, **2: 4**, 357-376.

Midorikawa, S. and Ohtake, Y. (2003). Empirical Analysis of Variance of Ground Motion Intensity inAttenuation Relationships, *Journal of Japan Association for Earthquake Engineering*, **3: 1**, 59-70. (in Japanese with Engilish abstract)

Strasser, F. O. and Bommer, J. J. (2005). Preliminary Simulation with EXWIM: Calibration and Assessment of Ground-Motion Variability in the Near-Source Region, Research report number: 05-002-SM, Imperial College London.

Tanaka, K., Wang, M. and Takada, T. (2008). Covariance Structure between Spectral Accelerations with Different Periods and its Appllications, *Journal of structural and construction engineering. Transactions of AIJ*, **73: 632**, 1727-1733. (in Japanese with Engilish abstract)

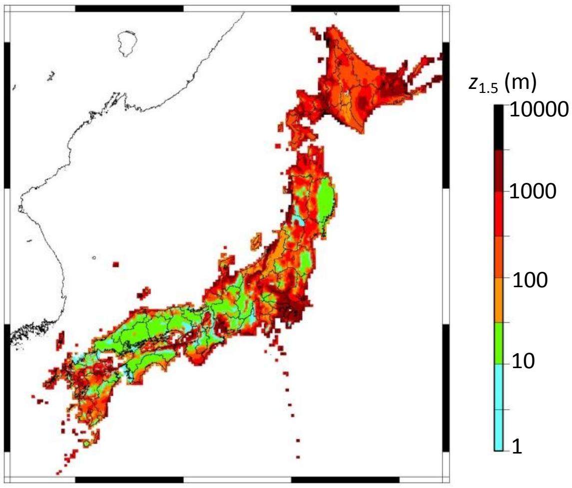

Figure 9. Depth of rock with shear wave velocity 1.5km/s ($z_{1.5}$) obtained from subsurface structure model in Japan proposed by Fujiwara et al. (2009a) (from Itoi & Takada, 2011)

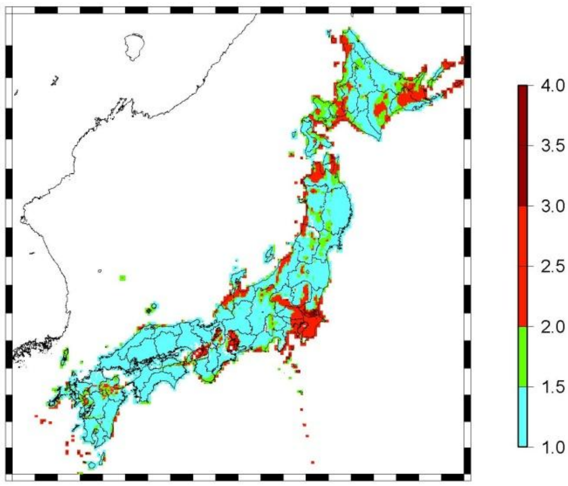

Figure 10. Spectral amplification (T=3.0 s) in Japan calculated by one-dimensional multiple reflection theory from seismic bedrock to engineering bedrock (Itoi & Takada, 2011)

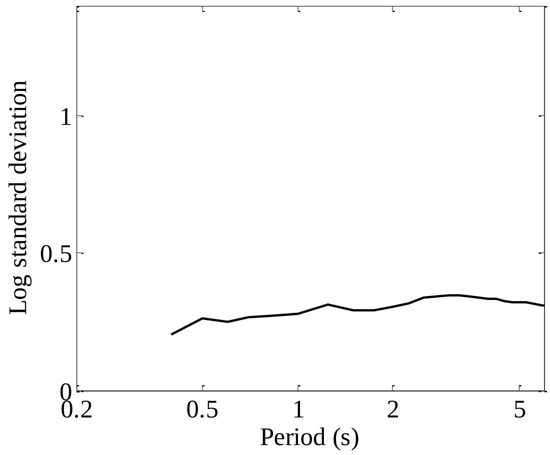

Figure 11. Standard deviation of ground motion variation due to deep subsurface structure based on ground motion simulation

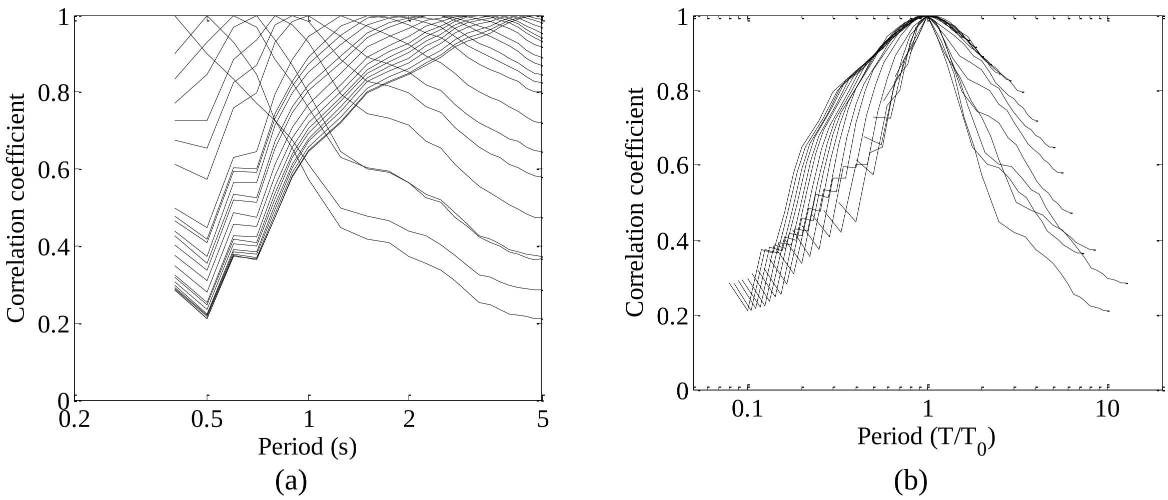

Figure 12. Correlation coefficients of response spectra due to deep subsurface structure based on ground motion simulation

Uchiyama, Y. and Midorikawa, S. (2006). Attenuation Relationship for Response Spectra on Engineering Bedrock Considering Effects of Focal Depth, *Journal of structural and construction engineering, Transactions of AIJ*, **(606)**, 81-88.

Wang, M. (2007). *New Perspectives for Probabilistic Prediction of Seismic Ground Motion*, PhD dissertation, The University of Tokyo.

Wang, M., Tanaka, K. and Takada, T. (2009). *Probabilistic seismic risk analysis for building portfolio, Safety, Reliability anb Risk of Structures, Infrastructures and Engineering Systems, Proceedings of 10th International Conference on Structural Safety and Reliability*, 2148-2155.